Electronic Supplementary Material (ESI) for Environmental Science: Atmospheres.

Supplementary material

Table S1: Measurements sites included from the ARPAE (Italy) and NABEL (Switzerland) networks*.

Station name	Region	Longitude (deg)	Latitude (deg)	Station type
Flaminia	ARPAE	12,6	44,1	urban
Marecchia	ARPAE	12,6	44,1	urban
San Clemente	ARPAE	12,6	43,9	rural
San Leo	ARPAE	12,4	43,9	rural
Cittadella	ARPAE	10,3	44,8	urban
Montebello	ARPAE	10,3	44,8	urban
Badia	ARPAE	10,3	44,7	rural
Saragat	ARPAE	10,4	44,9	suburban
Castellarano	ARPAE	10,7	44,5	suburban
S. Lazzaro	ARPAE	10,7	44,7	urban
Febbio	ARPAE	10,4	44,3	rural
S. Rocco	ARPAE	10,7	44,9	rural
Timavo	ARPAE	10,6	44,7	urban
Giardini	ARPAE	10,9	44,6	urban
Remesina	ARPAE	10,9	44,8	suburban
Parco Ferrari	ARPAE	10,9	44,7	urban
San Francesco	ARPAE	10,8	44,5	urban
Gavello	ARPAE	11,2	44,9	rural
Parco Edilcarani	ARPAE	10,8	44,5	urban
Lugagnano	ARPAE	9,8	44,8	suburban
Giordani-Farnese	ARPAE	9,7	45,0	urban
Besenzone	ARPAE	10,0	45,0	rural
Parco Montecucco	ARPAE	9,7	45,0	urban
Corte Brugnatella	ARPAE	9,4	44,7	rural
Parco Resistenza	ARPAE	12,0	44,2	urban
Roma	ARPAE	12,1	44,2	urban
Franchini-Angeloni	ARPAE	12,2	44,1	urban
Savignano	ARPAE	12,4	44,1	suburban
Savignano Di Rigo	ARPAE	12,2	43,9	rural
De Amicis	ARPAE	11,7	44,4	urban
Giardini Margherita	ARPAE	11,4	44,5	urban
Porta San Felice	ARPAE	11,3	44,5	urban
San Lazzaro	ARPAE	11,4	44,5	urban
San Pietro Capofiume	ARPAE	11,6	44,7	rural
Via Chiarini	ARPAE	11,3	44,5	suburban
Castelluccio	ARPAE	10,9	44,1	rural
Isonzo	ARPAE	11,6	44,8	urban
Gherardi	ARPAE	12,0	44,8	rural

Cento	ARPAE	11,3	44,7	suburban
Villa Fulvia	ARPAE	11,6	44,8	urban
Ostellato	ARPAE	11,9	44,7	rural
Zalamella	ARPAE	12,2	44,4	urban
Caorle	ARPAE	12,2	44,4	urban
Ballirana	ARPAE	12,0	44,5	rural
Delta Cervia	ARPAE	12,3	44,3	suburban
Parco Bertozzi	ARPAE	11,9	44,3	urban
Bern-Bollwerk	NABEL	7,4	47,0	urban
Lausanne-César-Roux	NABEL	6,6	46,5	urban
Lugano-Università	NABEL	9,0	46,0	urban
Zürich-Kaserne	NABEL	8,5	47,4	urban
Basel-Binningen	NABEL	7,6	47,5	suburban
Dübendorf-Empa	NABEL	8,6	47,4	suburban
Härkingen-A1	NABEL	7,8	47,3	ruralA
Sion-Aéroport-A9	NABEL	7,3	46,2	ruralAuto
Magadino-Cadenazzo	NABEL	8,9	46,2	ruralU1000
Payerne	NABEL	6,9	46,8	ruralU1000
Tänikon	NABEL	8,9	47,5	ruralU1000
Beromünster	NABEL	8,2	47,2	ruralU1000
Chaumont	NABEL	7,0	47,0	ruralO1000
Rigi-Seebodenalp	NABEL	8,5	47,1	ruralO1000
Davos-Seehornwald	NABEL	9,9	46,8	ruralO1000
Jungfraujoch	NABEL	8,0	46,5	mountain

* Station classified as mountain and above 1000 meters where not included in the analysis. *RuralA* refers to rural sites close to highways, whereas *ruralU1000* and *ruralO1000* refers to rural sites below and above 1000 meters, respectively.

Table S2: Definition of statistical metrics for model performance evaluation. *Mi* and *Oi* stand for modeled and observed values, respectively, and *N* is the total number of paired values. The Pearson correlation coefficient is calculated for the temporal variability.

Metric	Definition
Mean Bias (MB)	$MB = \frac{1}{N}\sum_{i=1}^{N}(M_i - O_i)$
Mean gross error (MGE)	$MGE = \frac{1}{N}\sum_{i=1}^{N}\left\|M_i - O_i\right\|$
Mean gross error (MGE)	$RMSE = \sqrt{\frac{1}{N}\sum_{i=1}^{N}(M_i - O_i)^2}$
Index of agreement (IOA)	$IOA = 1 - \frac{N \cdot RMSE^2}{\sum_{i=1}^{N}(\left\|M_i - \bar{O}\right\| + \left\|O_i - \bar{O}\right\|)^2}$
Pearson correlation coefficient (r)	$r = \frac{\sum_{i=1}^{N}(M_i - \bar{M}) \cdot (O_i - \bar{O})}{\sqrt{\sum_{i=1}^{N}(M_i - \bar{M})^2} \cdot \sqrt{\sum_{i=1}^{N}(O_i - \bar{O})^2}}$
Mean fractional bias (MFB)	$MFB = \frac{1}{N}\sum_{i=1}^{N}\frac{2 \cdot (M_i - O_i)}{M_i + O_i}$
Mean fractional error (MFE)	$MFE = \frac{1}{N}\sum_{i=1}^{N}\frac{2 \cdot \left\|(M_i - O_i)\right\|}{M_i + O_i}$
Absolute change	(CAMx-COVID – CAM-BAU)
Relative change	((CAMx-COVID – CAM-BAU)/CAMx-BAU)

Table S3: Performance criteria and goals for model results (Boylan and Russell, 2006; EPA, 2007).

Parameter	Metric	Criteria	Goal
$PM_{2.5}$	MFB MFE	≤ ±60 % ≤ 75 %	≤ ±30 % ≤ 50 %
O_3	MFB MFE	≤ ±30 % ≤ 45 %	≤ ±15 % ≤ 30 %

Table S4: Chemical reactions tagged with the Process analysis tool (Ramboll, 2018).

Reactions (ppb h^{-1})	Description
HNO_3-prod	Nitric acid total production rate
$\cdot NO_3$-prod	Nitrate radical total production rate
$N_2O_5wH_2O$	Nitric acid production rate via heterogeneous reaction
NO_2wOH	Nitric acid production rate via NO_2 oxidation by ·OH radical
OHwVOC	VOC reactions rate with ·OH radical
NO_3wVOC	VOC reactions rate with $\cdot NO_3$ radical
·OH-prod	Total production rate of ·OH radical
$\cdot HO_2$-prod	Total production rate of $\cdot HO_2$ radical
·OH-photolysis	·OH from photolysis processes
$O(^1D)+H_2O$	·OH from reactions of oxygen in the excited states with water
O_3+VOCs	·OH from the reactions of O_3 with VOCs

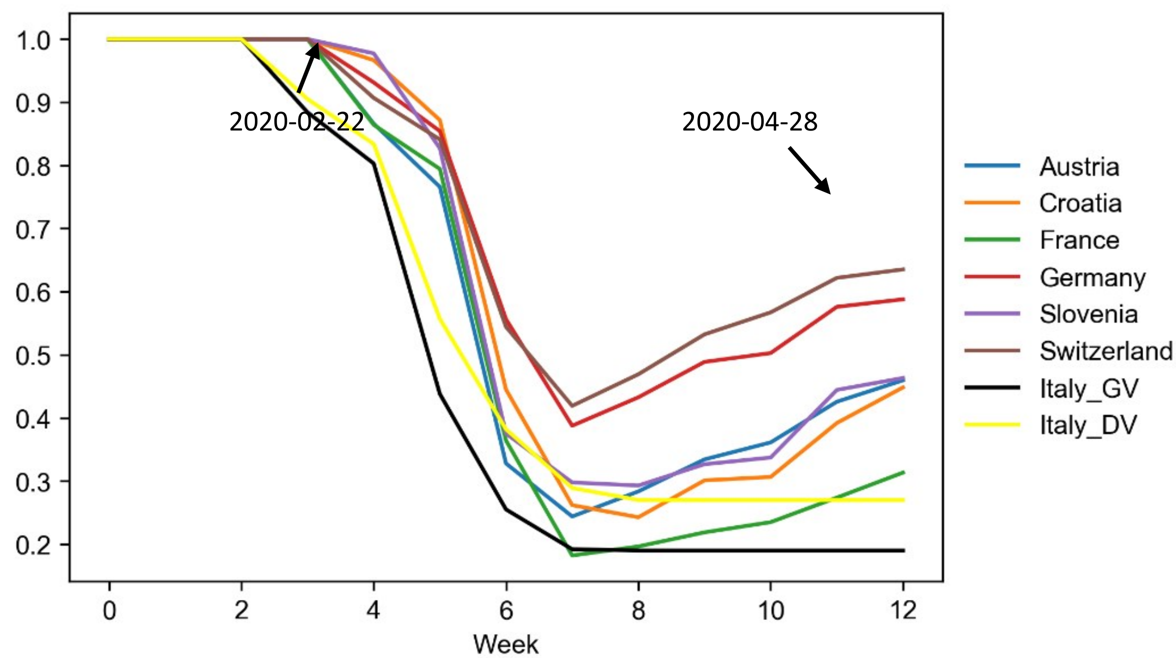

Figure S1: Scaling factors for emissions in CAMx-LOCK scenario. GV and DV represent gasoline and diesel vehicles, respectively.

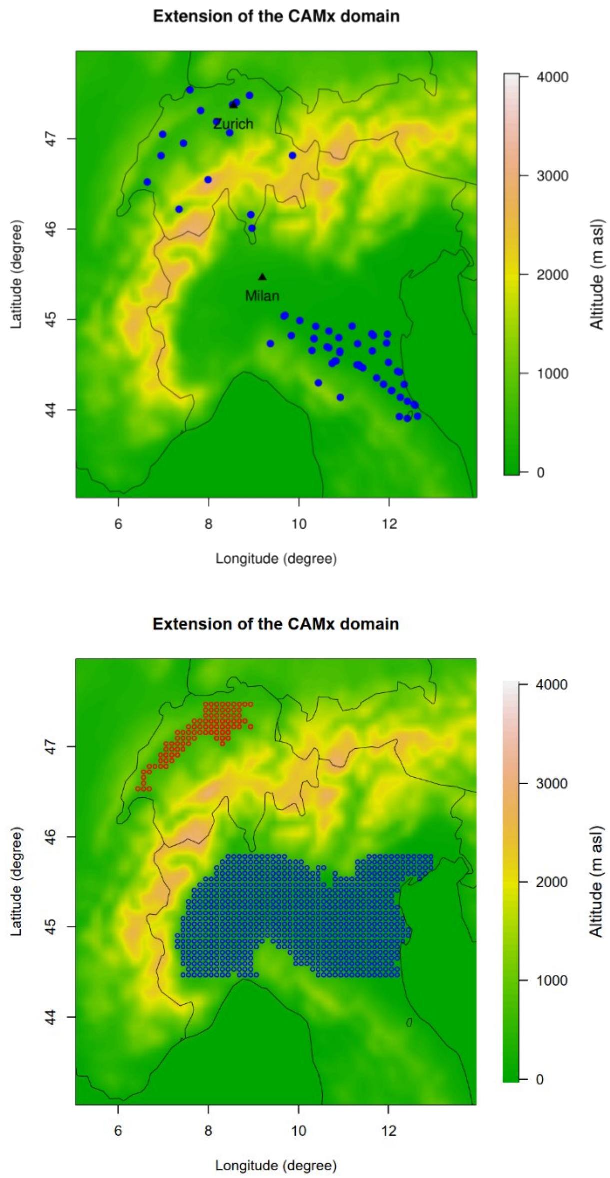

Figure S2: Locations of the measurement sites (ARPAE and NABEL stations) included in the analysis (left) and model cells used to retrieve the Swiss Plateau (red circles) and Po Valley (blue circles) regions.

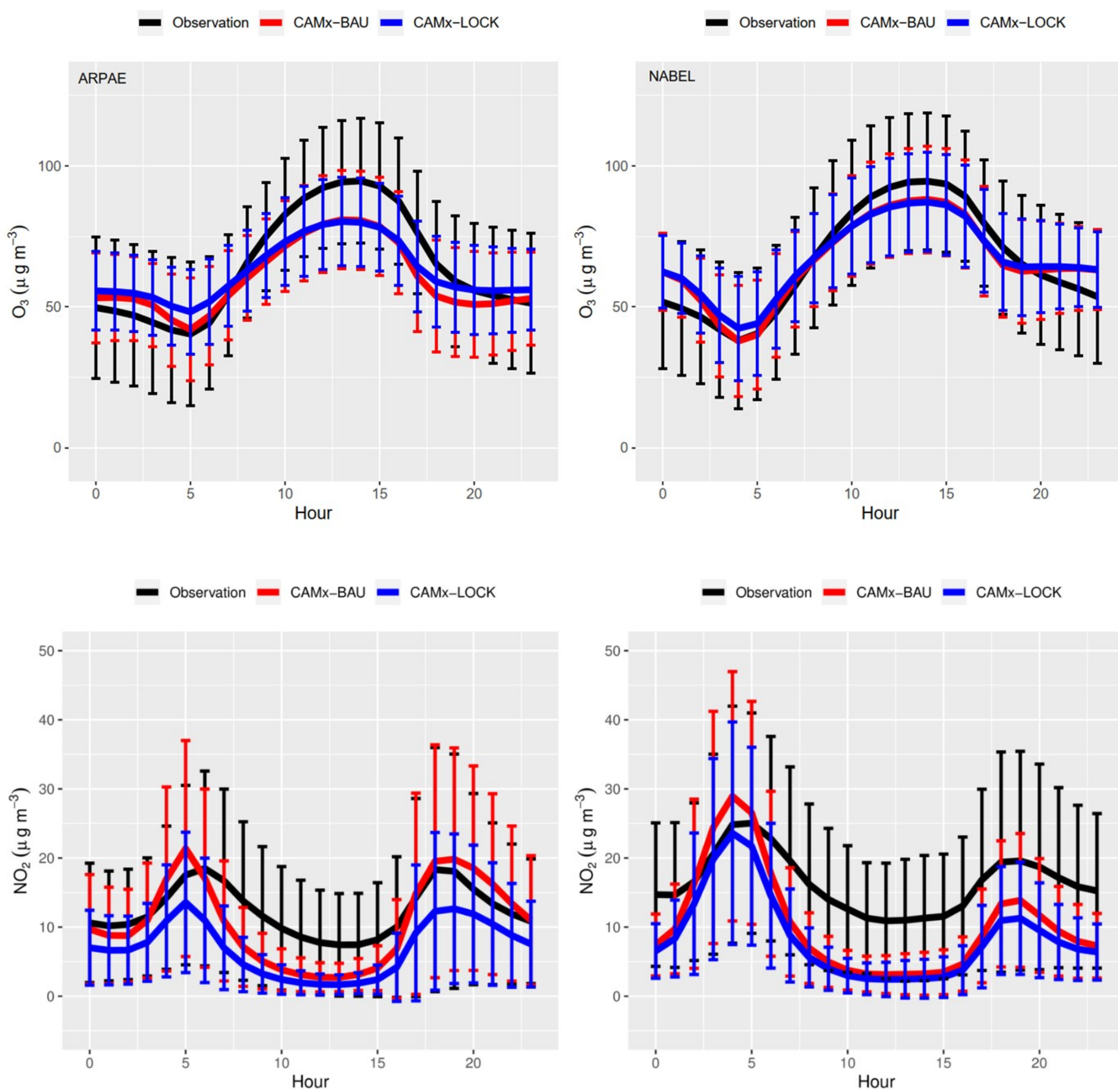

Figure S3: Diurnal cycles (UTC) of O_3 (top panel) and NO_2 (bottom panel) concentrations for the ARPAE (left panels) and NABEL stations (right panels) (8 March – 27 April 2020).

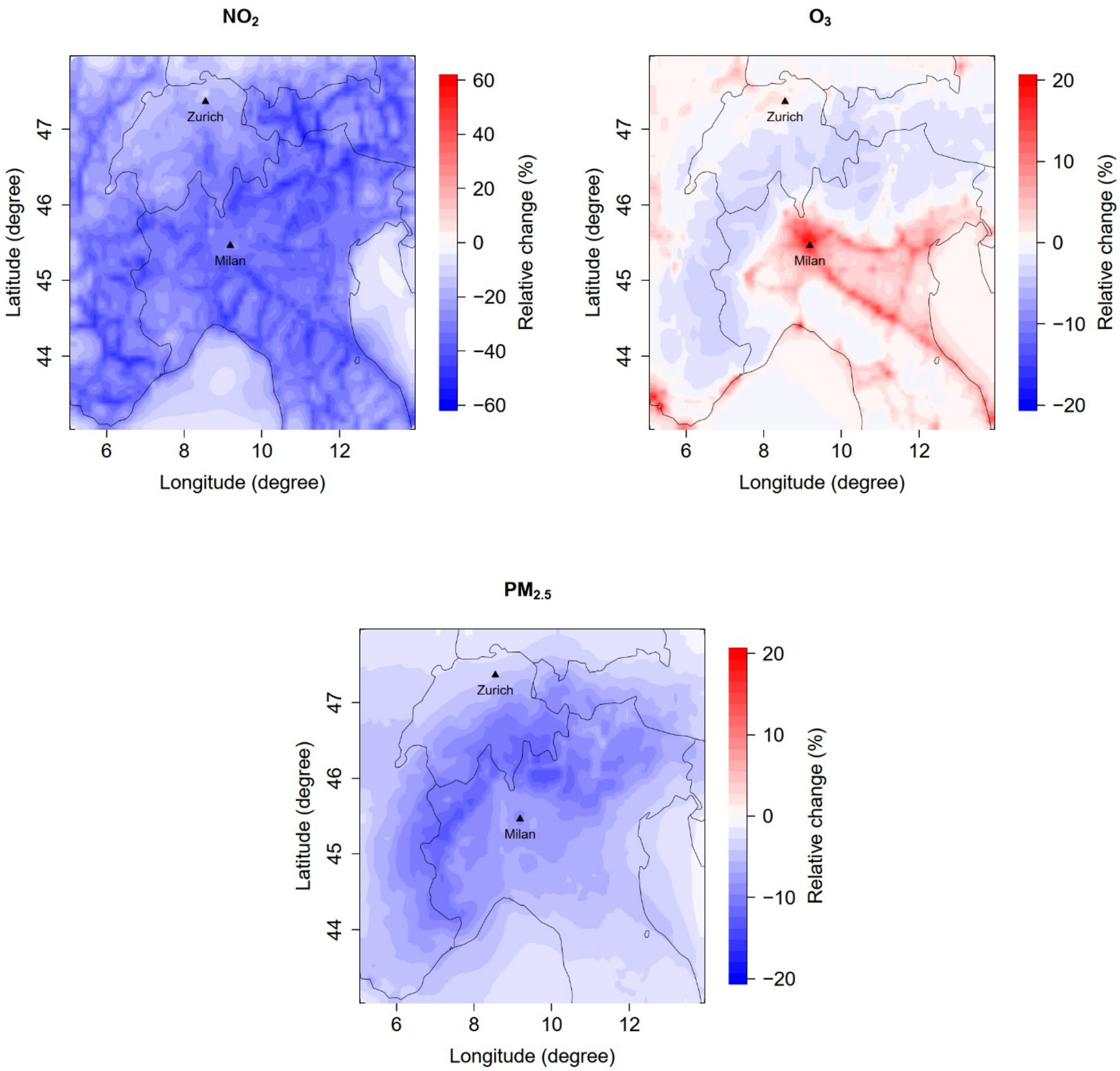

Figure S4: Modeled NO_2, O_3, and $PM_{2.5}$ average relative changes over the CAMx domain (8 March – 27 April 2020).

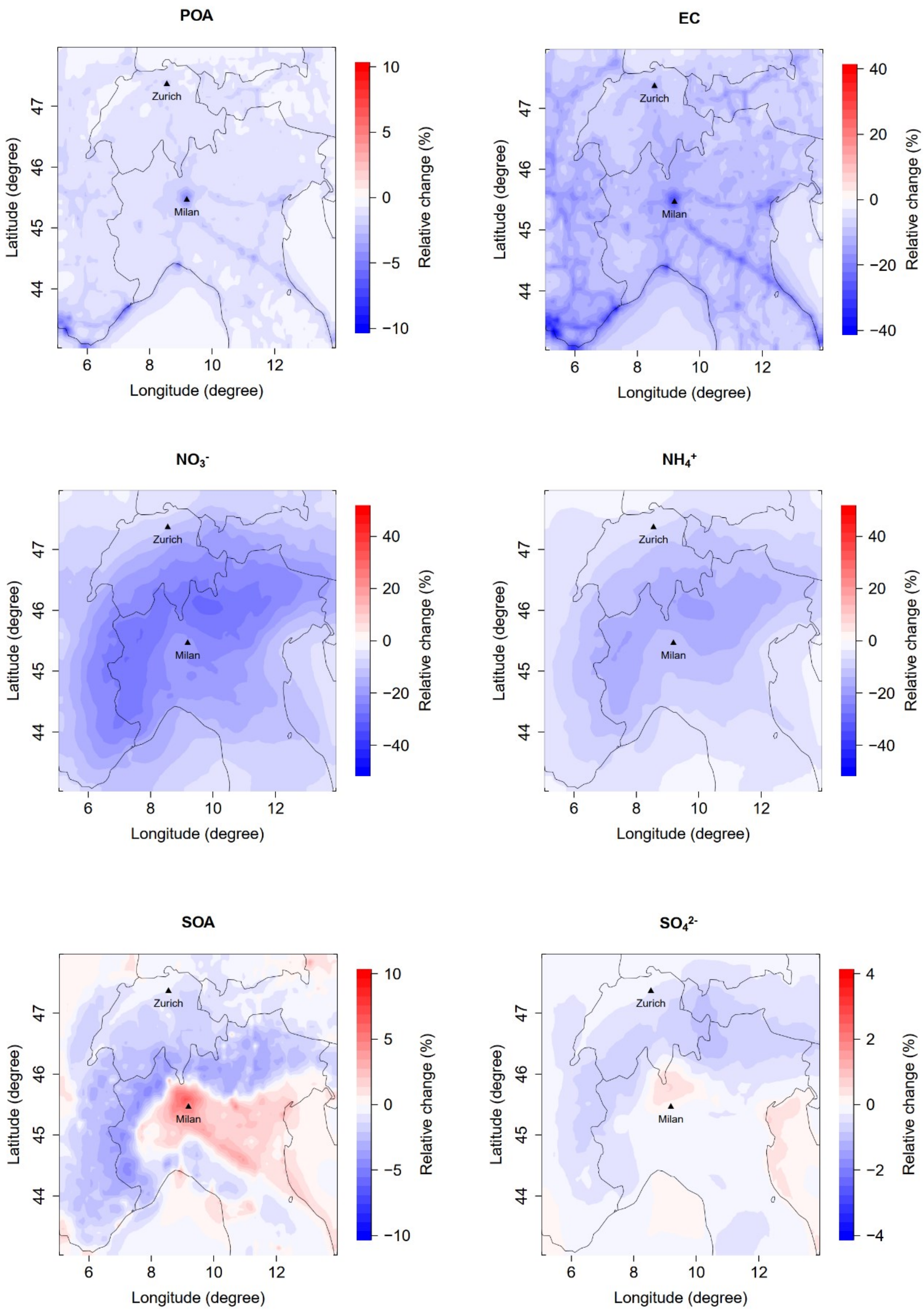

Figure S5: Relative changes in POA, EC, NO_3^-, NH_4^+, SO_4^{2-} and SOA concentrations over the CAMx domain (8 March – 27 April 2020).

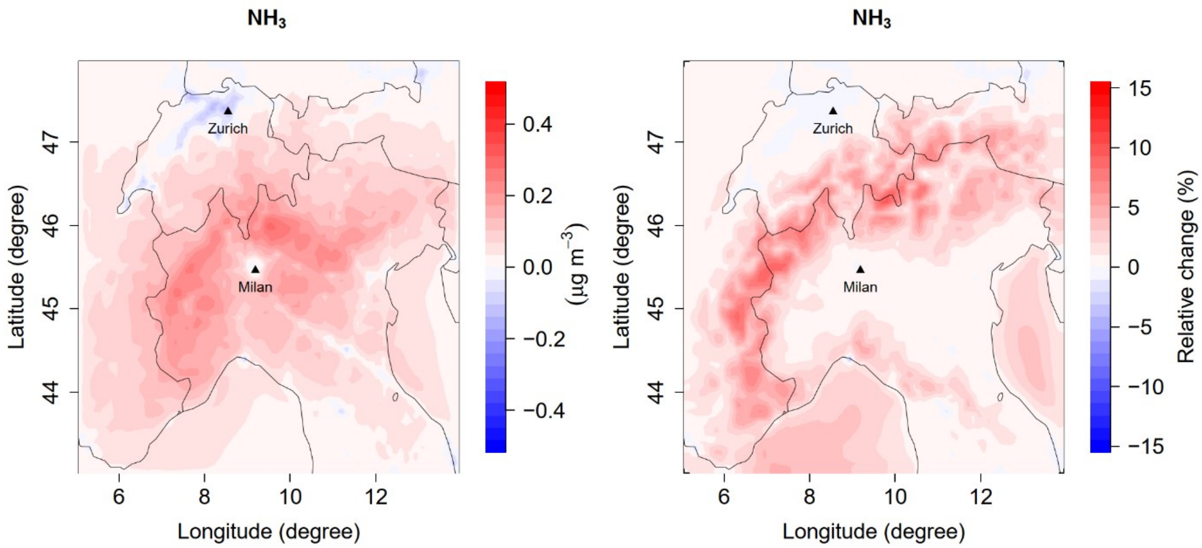

Figure S6: Modeled NH_3 absolute changes (i.e. CAMx-LOCK – CAMx-BAU, left-panel) and relative changes, right-panel (8 March – 27 April 2020).

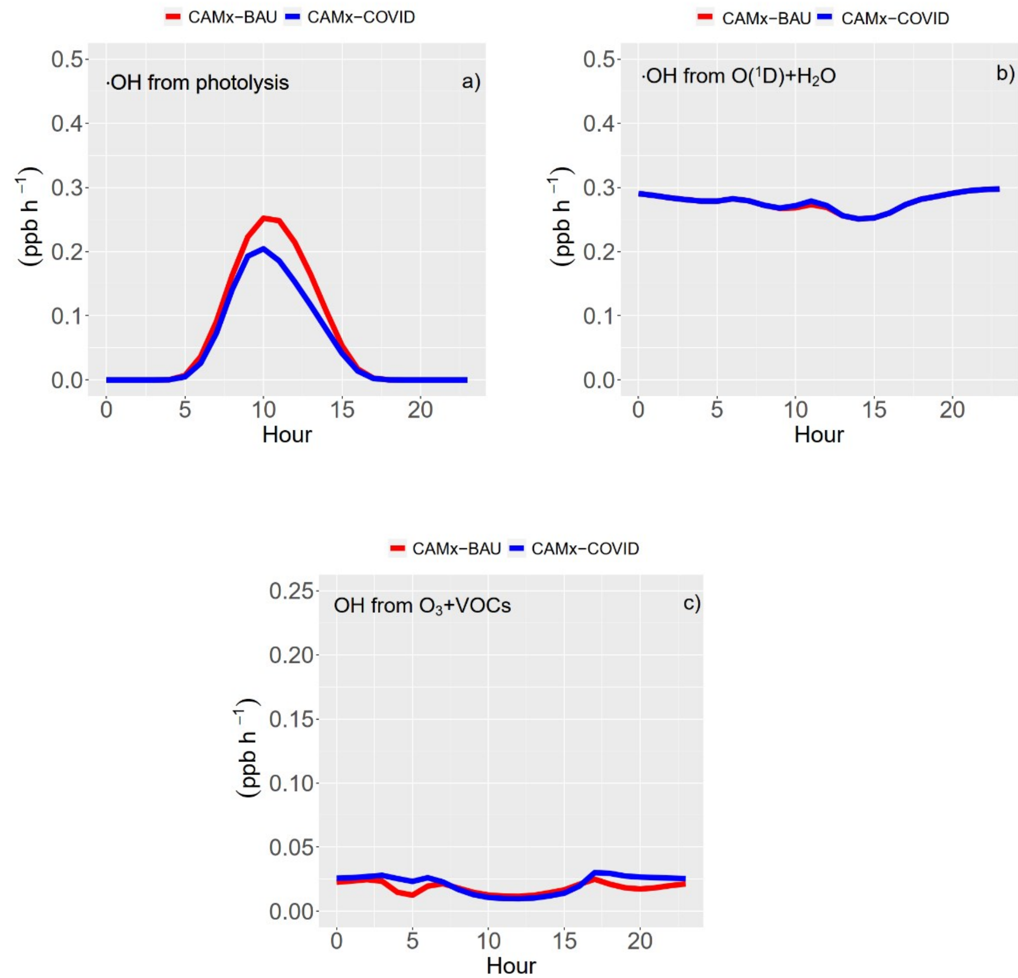

Figure S7: Direct sources of ·OH radicals in the CAMx-BAU and CAMx-COVID scenarios. ·OH-photolysis (a) includes the photolysis of HONO, HNO_3, and H_2O_2 as well as methylhydroperoxide, peroxyacetic, higher peroxycarboxylic acids and higher organic peroxide. Units are in ppb h^{-1}.

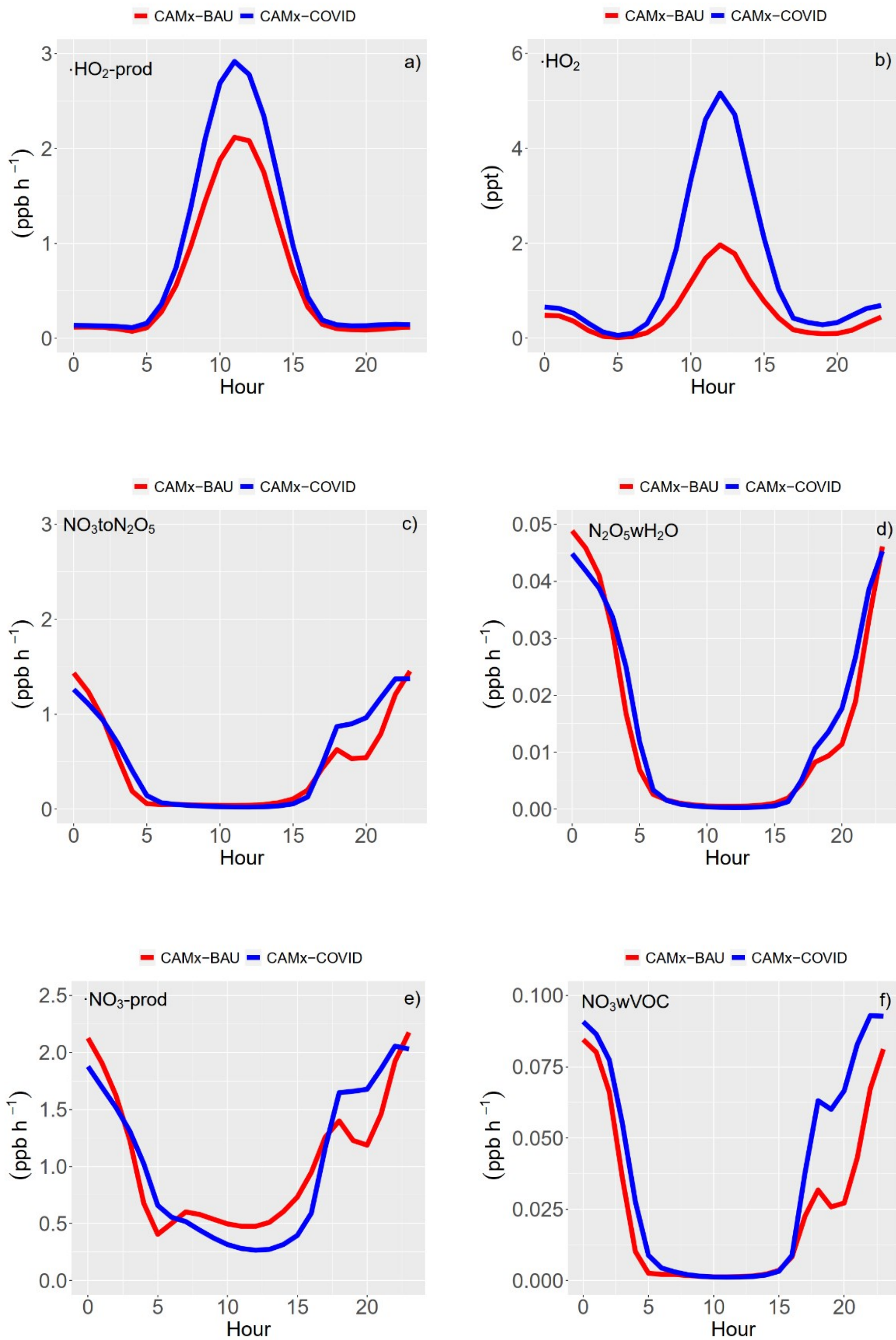

Figure S8: Diurnals variations of $\cdot HO_2$-prod (a), $\cdot HO_2$ (b), $NO_3toN_2O_5$ (c), $N_2O_5wH_2O$ (d), NO_3-prod (e) and NO_3wVOC (f) over the "Greater Milan" area (8 March – 27 April 2020). Units are in ppb h^{-1} for the reactions and in ppt for the $\cdot OH_2$ concentrations.

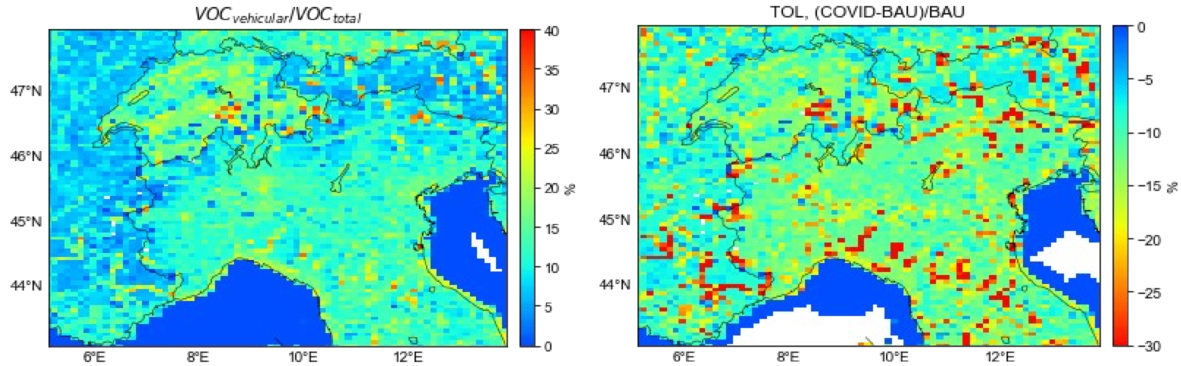

Figure S9: Contribution of vehicular VOCs to the total VOCs emissions (left panel), and relative changes in toluene emissions between the BAU and the COVID scenarios (right panel) due to the reduced traffic emissions.